Controllable single-photon transport in an optical waveguide coupled to an optomechanical cavity with a V-type three-level atom

Yuqing Zhang (张玉青)[1,*], Zhonghua Zhu (朱中华)[1], Zhaohui Peng (彭朝晖)[1], Chunlei Jiang (姜春蕾)[1], Yifeng Chai (柴一峰)[1], and Lei Tan (谭 磊)[2]

[1]*School of Physics and Electronic Science, Hunan University of Science and Technology, Xiangtan 411201, China*
[2]*Institute of Theoretical Physics, Lanzhou University, Lanzhou 730000, China*
**Corresponding author: lanzhougx@163.com*

Received July 31, 2017; accepted October 13, 2017; posted online November 6, 2017

An optomechanical cavity embedded with a V-type three-level atom is exploited to control single-photon transport in a one-dimensional waveguide. The effects of the atom–cavity detuning, the optomechanical effect, the coupling strengths between the cavity and the atom or the waveguide, and the atomic dissipation on the single-photon transport properties are analyzed systematically. Interestingly, the single-photon transmission spectra show multiple double electromagnetically induced transparency. Moreover, the double electromagnetically induced transparency can be switched to a single one by tuning the atom–cavity detuning.

OCIS codes: 270.1670, 270.5580, 020.5580, 020.1670.
doi: 10.3788/COL201816.012701.

Single-photon transport in waveguide quantum electrodynamics systems coupled with atoms or quantum dots has stimulated considerable interest because of its important applications in quantum computation, quantum information processing, and the realization of all-optical quantum devices[1–12]. Recently, cavity optomechanics has opened the prospect of manipulating the propagating single photon[13–18]. It has wide applications, such as in ultrasensitive measurements of the position of a mirror, allowing for gravitational wave detection[19,20], realization of macroscopic quantum objects[21], and as a fundamental platform for exploring coupling to other quantum systems[22].

With the rapid advance in optical trapping and microfabrication techniques, cavity optomechanics has entered the single-photon strong coupling regime[23,24]. Therefore, it is convenient to control the single-photon transport in a waveguide by means of cavity optomechanics. Based on the model of a single-mode fiber coupled to an empty optomechanical cavity, Ren *et al.*[25] derived single-photon transmission amplitudes with a real-space approach and explored the influences of the optomechanical cavity and mechanical dissipation on the photon transport. Jia's group[26] reported a single photon scattered by an optomechanical cavity embedded with a two-level atom coupled to a one-dimensional waveguide. An analogous Rabi splitting and electromagnetically induced transparency (EIT) -like phenomena in the single-photon spectra were observed in different parameter regimes. It should be interesting to introduce a multilevel emitter, such as a three-level atom in such a system. Then, more controllable parameters to manipulate the single-photon behavior could be provided, and, hence, rich physical phenomena are expected[27–29]. In this work, we investigate a controllable single-photon transport in a one-dimensional waveguide, side-coupled to an optomechanical cavity with a V-type three-level atom (VTA). Our results demonstrate that the transmission spectra in the considered system show multiple EIT phenomena. The effects of the single-photon optomechanical coupling strength, the optomechanics–waveguide coupling strength, the interaction between the atom and the cavity, as well as the atom–cavity detuning on the single-photon properties are discussed. In addition, the influence of the atomic dissipation on the single-photon transport is explored.

We consider an optical waveguide coupled to an optomechanical cavity with a VTA inside. The sketch and atomic-level structure are shown in Fig. 1. The Hamiltonian of the system is given by ($\hbar = 1$)

$$\begin{aligned} H = & \int \mathrm{d}x a_R^+(x)\left(-iv_g\frac{\partial}{\partial x}\right)a_R(x) \\ & + \int \mathrm{d}x a_L^+(x)\left(iv_g\frac{\partial}{\partial x}\right)a_L(x) + \omega_1\sigma_{11} + (\omega_2 - i\gamma_2)\sigma_{22} \\ & + (\omega_3 - i\gamma_3)\sigma_{33} + \omega_c c^+c + \Omega b^+b - g_0 c^+c(b + b^+) \\ & + \lambda_1(c\sigma_{31} + c^+\sigma_{13}) + \lambda_2(c\sigma_{21} + c^+\sigma_{12}) \\ & + V\int \mathrm{d}x\delta(x)[a_R^+(x)c + a_R(x)c^+ + a_L^+(x)c \\ & + a_L(x)c^+], \end{aligned} \tag{1}$$

where $a_R^+(x)[a_R(x)]$ and $a_L^+(x)[a_L(x)]$ are the bosonic creation (annihilation) operators of the right- and left-going photons with group velocity v_g at position x, respectively. The energies of the levels $|i\rangle$ $(i = 1, 2, 3)$ are $\hbar\omega_i$. $\sigma_{\mu\nu} = |\mu\rangle\langle\nu|$ $(\mu, \nu = 1, 2, 3)$ is the transition operator between μ and ν. γ_2 and γ_3 describe the atomic dissipation rates.

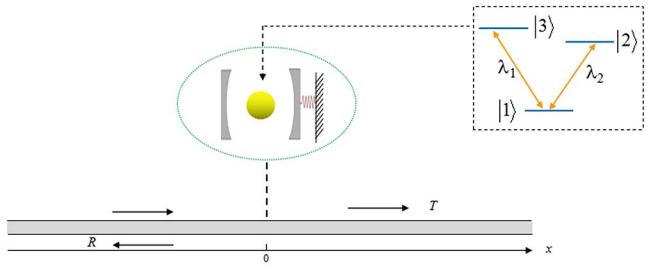

Fig. 1. Schematic diagram of a hybrid atom–optomechanical system interacting with an optical waveguide. The hybrid system consists of an optomechanical cavity and a VTA, and the single-photon travels along the arrow direction in the one-dimensional optical waveguide.

$c^+(b^+)$ is the photon (phonon) creation operator. ω_c and Ω are the optomechanical cavity and the mechanical mode resonance frequencies, respectively. g_0 is the single-photon coupling strength between the cavity and the mechanical mode. λ_1 and λ_2 describe the interaction between the VTA and the optomechanical cavity associated with the atomic transitions $|1\rangle$–$|3\rangle$ and $|1\rangle$–$|2\rangle$, respectively. V denotes the coupling strength between the cavity and the waveguide. $\delta(x)$ implies that the interaction occurs only at $x = 0$. The decay rate of the photon from the optomechanical cavity into the waveguide is given as $\Gamma = V^2/\upsilon_g$.

When a single photon comes into a one-dimensional optical waveguide, the stationary eigenstate in the single-photon subspace for the total Hamiltonian can be expressed as

$$\begin{aligned}|\psi\rangle = &\sum_n \int \mathrm{d}x[\phi_R(x,n)a_R^+(x)|\varnothing\rangle|n\rangle_b \\ &+ \phi_L(x,n)a_L^+(x)|\varnothing\rangle|n\rangle_b] \\ &+ \sum_n a_n c^+|\varnothing\rangle|\tilde{n}\rangle_b + \sum_n b_n\sigma_{21}|\varnothing\rangle|n\rangle_b \\ &+ \sum_n c_n\sigma_{31}|\varnothing\rangle|n\rangle_b, \end{aligned} \tag{2}$$

where $\phi_R(x,n)$ and $\phi_L(x,n)$ denote the probability amplitudes of the right- and left-propagating photons, respectively. $|\varnothing\rangle$ denotes that there are no photons in both the waveguide and the cavity, as well as the atom in the ground state. $|n\rangle_b$ represents the number state of the mechanical mode. a_n describes the excitation amplitude of the cavity. b_n and c_n are the probability amplitudes of the atomic states $|2\rangle$ and $|3\rangle$, respectively. $|\tilde{n}\rangle_b = \exp[g_0(b^+ - b)/\Omega]|n\rangle_b$ is the single-photon displaced number state of the mechanical oscillator, satisfying the eigen equation

$$\begin{aligned}&[\omega_c c^+c + \Omega b^+b - g_0 c^+c(b+b^+)]|1\rangle_c|\tilde{n}\rangle_b \\ &\quad = (\omega_c + n\Omega - \delta)|1\rangle_c|\tilde{n}\rangle_b, \end{aligned} \tag{3}$$

with the photon-state frequency $\delta = g_0^2/\Omega$. $\phi_{R,L}(x,n)$ are given by

$$\phi_R(x,n) = [\theta(-x)\delta_{\mathrm{nn}_0} + \theta(x)t_n]e^{i\left[k+(n_0-n)\frac{\Omega}{\upsilon_g}\right]x}, \tag{4}$$

$$\phi_L(x,n) = \theta(-x)r_n e^{-i\left[k+(n_0-n)\frac{\Omega}{\upsilon_g}\right]x}. \tag{5}$$

For simplicity, we assume that the initial state of the mechanical resonator is in number state $|n_0\rangle_b$ and let $n_0 = 0$ to get numeric results. By solving the eigen equation $H|\psi\rangle = E|\psi\rangle$, we can therefore obtain a set of equations, expressed as follows:

$$-i\upsilon_g(t_n - \delta_{\mathrm{nn}_0}) + V\sum_m a_m U_{\mathrm{nm}} = 0, \tag{6}$$

$$-i\upsilon_g r_n + V\sum_m a_m U_{\mathrm{nm}} = 0, \tag{7}$$

$$\frac{V}{2}(\delta_{\mathrm{nn}_0} + t_n + r_n) + \lambda_1 c_n + \lambda_2 b_n = \sum_m \tilde{\Delta}_c(m)a_m U_{\mathrm{nm}}, \tag{8}$$

$$\lambda_2\sum_m a_m U_{\mathrm{nm}} = \tilde{\Delta}_{a1}(n)b_n, \tag{9}$$

$$\lambda_1\sum_m a_m U_{\mathrm{nm}} = \tilde{\Delta}_{a2}(n)c_n, \tag{10}$$

with $\tilde{\Delta}_c(m) = \Delta_c + (n_0 - m)\Omega + \delta$, $\tilde{\Delta}_{a1}(n) = \Delta_c - \Delta_{\mathrm{ac1}} + (n_0 - n)\Omega + i\gamma_2$, $\tilde{\Delta}_{a2}(n) = \Delta_c - \Delta_{\mathrm{ac2}} + (n_0 - n)\Omega + i\gamma_3$. $\Delta_{\mathrm{ac1}} = \omega_{12} - \omega_c$, $\Delta_{\mathrm{ac2}} = \omega_{13} - \omega_c$, and $\Delta_c = \upsilon_g k - \omega_c$ denote the detunings between the atom or the incident photon and the cavity, respectively. $U_{\mathrm{nm}} = \langle n|_b|\tilde{m}\rangle_b$, and $E = \upsilon_g k + n_0\Omega + \omega_1$. According to Eqs. (6)–(10), the photon's transmission and reflection spectra could be obtained through the relations $T = \sum_n |t_n|^2$, and $R = \sum_n |r_n|^2$. Based on the numerical results, we will discuss the coherent transport properties of the single photon by controlling the parameters of the optomechanical cavity and the VTA.

Firstly, we explore the influence of the atom–cavity detuning. The group velocity of the photon is chosen as $\upsilon_g = 1$ for numerical investigation. Figure 2 presents the single-photon transmission spectra for different atom–cavity detunings in the absence of the optomechanical effect (i.e., $g_0 = 0$). When $\Delta_{\mathrm{ac1}} = \Delta_{\mathrm{ac2}} = 0$, as shown in Fig. 2(a), a typical EIT is exhibited in the transmission spectrum. With the atom–cavity detunings $\Delta_{\mathrm{ac1}} = 0$, but $\Delta_{\mathrm{ac2}} \neq 0$, the spectra show an interesting double EIT, consisting of three dips and double peaks in the transmission spectrum, as depicted in Figs. 2(b)–2(d). Obviously, the two peaks are associated with the two transition paths of the three-level atom, which is confirmed by the results in Figs. 2(b)–2(j). As the detuning Δ_{ac2} increases, the peak on the right moves in the positive direction along the Δ_c axis, but the one on the left keeps still. In addition, for far detuning Δ_{ac2}, there is a recurrence of the single EIT, where the right peak located in the double EIT window is removed, as shown in Fig. 2(e). The results imply that a switch between a double EIT and a single one can be

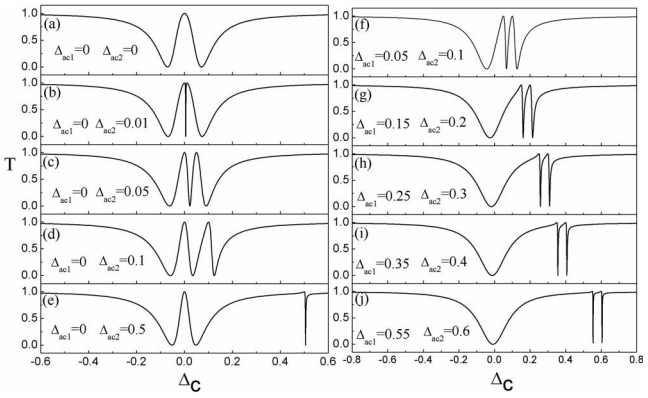

Fig. 2. Single-photon transmission spectra for different atom–cavity detunings. (a)–(e) $\Delta_{ac1} = 0$, and $\Delta_{ac2} \neq 0$. (f)–(j) $\Delta_{ac1} \neq 0$, and $\Delta_{ac2} \neq 0$. Other parameters: $g_0 = 0$, $\lambda_1 = \lambda_2 = 0.05$, $\gamma_2 = \gamma_3 = 0$, $\Gamma = 0.1$. All of the parameters are in units of Ω.

realized by tuning the atom–cavity detuning. The case of double atom–cavity detunings with $\Delta_{ac1} \neq 0$, and $\Delta_{ac2} \neq 0$ is also plotted in Figs. 2(f)–2(j). Figure 2(f) shows that the double peaks are not located in the center of the EIT window. When the two detunings increase simultaneously, the double peaks move away from the center and convert to dips, leaving a broad transmission dip, as depicted in Figs. 2(g)–2(j).

Next, we explore the influences of the optomechanical coupling strength g_0 on the transmission behavior of the injected photon, as shown in Fig. 3. For $g_0 = 0$, a double EIT appears in the symmetric spectrum, as shown in Fig. 3(a). When the optomechanical effect is considered ($g_0 \neq 0$), the spectra show a complex structure. Especially for $g_0 = 1$, an interesting multiple double EIT occurs in the transmission spectra, as depicted in Fig. 3(d). For the model of the two-level atom coupled to the optomechanical cavity, there are two kinds of dressed states ($|\psi_n^{(+)}\rangle$ and $|\psi_n^{(-)}\rangle$, $n = 0, 1, 2...$) in single-photon subspace (see Fig. 3 in Ref. [26]). In the regime $\lambda < \Gamma$, there is a

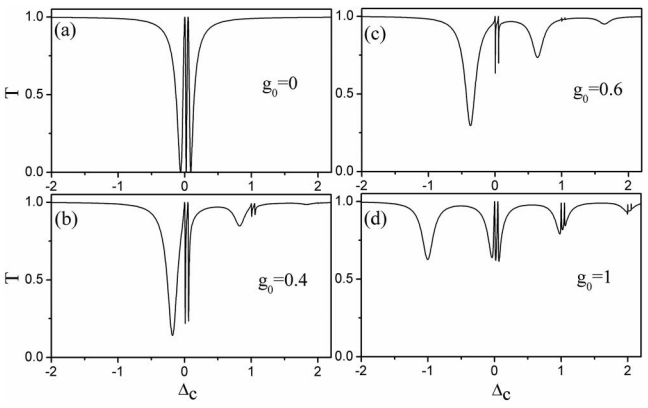

Fig. 3. Single-photon transmission spectra for different optomechanical coupling strengths. Other parameters: $\lambda_1 = \lambda_2 = 0.05$, $\Delta_{ac1} = 0$, $\Delta_{ac2} = 0.1$, $\gamma_2 = \gamma_3 = 0$, and $\Gamma = 0.1$. All of the parameters are in units of Ω.

destructive quantum interference between two transitions from the initial state ($|\mathbf{0}\rangle_c|\boldsymbol{g}\rangle_a|\mathbf{0}\rangle_b$) to the two near-degenerate dressed states ($|\boldsymbol{\psi}_n^{(+)}\rangle$ and $|\boldsymbol{\psi}_{n+m}^{(-)}\rangle$), and then a complete transmission of the single photon occurs, resulting in an EIT structure in the transmission spectra. Similarly, in this work, there should be three near-degenerate dressed states in the single-photon subspace, and then two different destructive quantum interferences occur, which leads to the formation of two peaks in the EIT windows. Moreover, when the optomechanical effect is considered, the photons along the waveguide interact with a series of energy sidebands, so multiple EITs would emerge in the single-photon transmission spectra.

Figure 4 displays how the coupling strength between the optomechanical cavity and the waveguide affects the single-photon transport. It is convenient to use Γ to characterize the coupling strength, since it describes the decay rate of spontaneous emission into the one-dimensional waveguide, which is given by $\Gamma = V^2/v_g$. As is seen from Fig. 4(a), when the interaction is very feeble, for example, $\Gamma = 0.01$, there are three narrow dips at around $\Delta_c = 0$. When the coupled system enters the region $(\lambda_1, \lambda_2) < \Gamma$, the transmission dip on the left is broadened gradually with increasing Γ. As a consequence, a double EIT structure emerges, which is composed of two sharp peaks and a very broad transmission dip. It is also noted that the two small peaks on the right are suppressed for a sufficiently strong coupling strength Γ, as demonstrated in Fig. 4(e). In this situation, $g_0 < \Gamma$, and the optomechanical effect is very weak.

Then, we pay attention to the effect of atom–cavity coupling strength on the single-photon spectra, as shown in Fig. 5. For simplicity, we fix $\lambda_2 = 0.05$ and change the value of λ_1. When λ_1 increases, the double EIT structure disappears gradually, and two splitting dips emerge in the

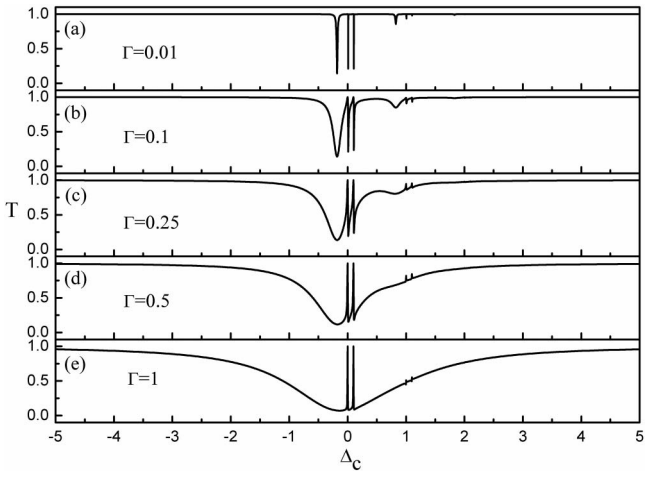

Fig. 4. Single-photon transmission spectra for various interaction strengths between the hybrid atom–optomechanical system and the waveguide. Other parameters: $g_0 = 0.4$, $\lambda_1 = \lambda_2 = 0.05$, $\Delta_{ac1} = 0$, $\Delta_{ac2} = 0.1$, $\gamma_2 = \gamma_3 = 0$. All of the parameters are in units of Ω.

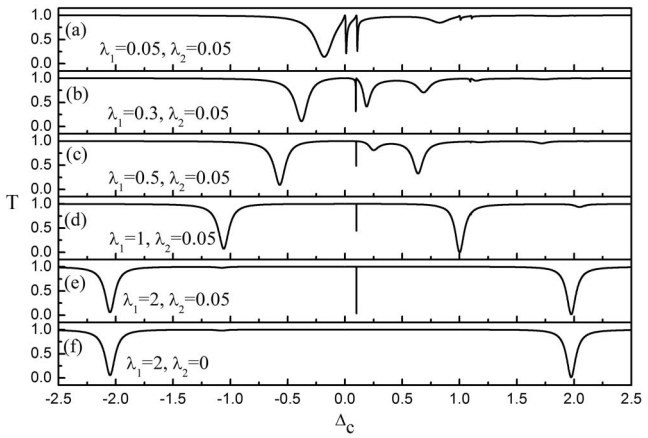

Fig. 5. Single-photon transmission spectra for various coupling strengths between the cavity and the VTA. Other parameters: $g_0 = 0.4$, $\Delta_{ac1} = 0$, $\Delta_{ac2} = 0.1$, $\gamma_2 = \gamma_3 = 0$, and $\Gamma = 0.1$. All of the parameters are in units of Ω.

spectra, as shown in Figs. 5(d) and 5(e). As is well-known, the structure of the single-photon spectra is decided by the relations among these parameters: λ, Γ, and Ω. When $\lambda < \Gamma$, the spectra show an EIT structure. But in the region $\lambda \gg \Omega \gg \Gamma$, strong atom–cavity coupling results in Rabi splitting of the spectra. Besides, there is an additional dip at around $\Delta_c = 0$ in the transmission spectra. However, when $\lambda_2 = 0$, the three-level atom is equivalent to a two-level atom, as plotted in Fig. 5(f). There are only two splitting dips in the transmission spectrum, showing vacuum Rabi splitting[26].

In a real system, the unavoidable loss always leads to the leakage of photons into non-waveguide channels. Here, the atomic loss ($\gamma_2 = \gamma_3 = 0.001$) in the present system is considered, as shown in Figs. 6 and 7. For the non-dissipation case in Fig. 6(a), the sum of the transmission and reflection probabilities is one (i.e., $R + T = 1$) due to no leakage of photons. When the dissipation is considered, it is less than one, as depicted in Fig. 6(b). In addition, as the coupling strength between the cavity and the atom increases, the effect of atomic dissipation is suppressed, and, then, the minima of $R + T$ get closer to one, as shown in Fig. 7.

In conclusion, we theoretically investigate the single-photon transport along a one-dimensional waveguide side-coupled to an optomechanical cavity embedded with a VTA. The influences of the atom–cavity detuning, the optomechanical effect, and the coupling strengths between the cavity and the atom or the waveguide on the transmitted spectra are discussed. It is found that, different from the case of a two-level atom, the transmission spectra in the considered system show multiple double EIT phenomena in a multiphonon process. By adjusting the atom–cavity detunings, a switch between a double EIT and a single EIT can be realized. Furthermore, it is shown that increasing the atom–cavity coupling strength could weaken the effect of atomic loss.

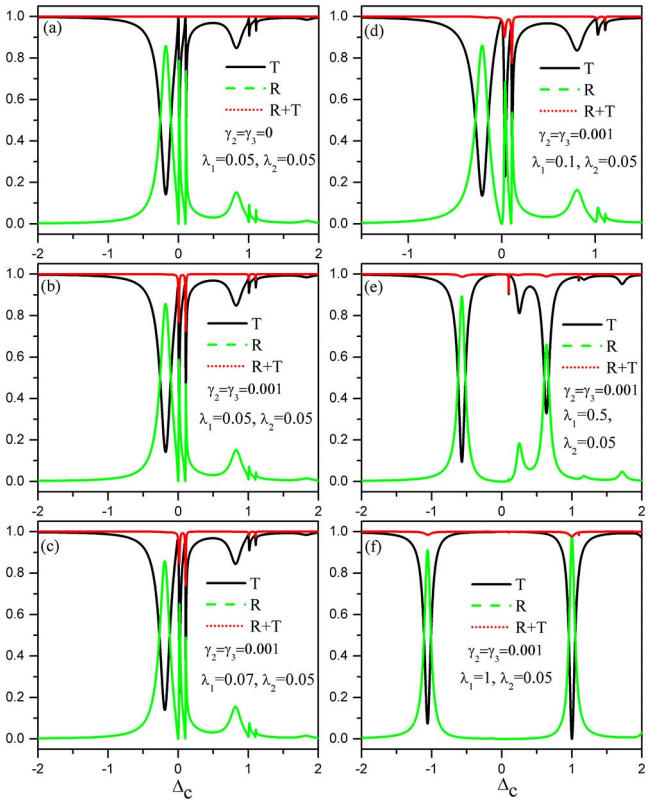

Fig. 6. (Color online) Single-photon transmission and reflection spectra in atomic dissipation and non-dissipation cases for various coupling strengths between the cavity and the VTA. (a) $\gamma_2 = \gamma_3 = 0$. (b)–(f) $\gamma_2 = \gamma_3 = 0.001$. Other parameters: $g_0 = 0.4$, $\Delta_{ac1} = 0$, $\Delta_{ac2} = 0.1$, and $\Gamma = 0.1$. All of the parameters are in units of Ω.

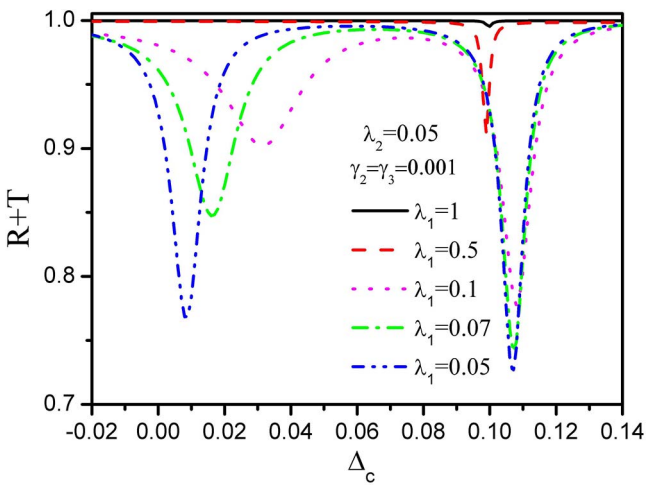

Fig. 7. (Color online) Sum of transmission and reflection probabilities of the single photon in atomic dissipation for various coupling strengths between the cavity and the three-level atom. Other parameters: $g_0 = 0.4$, $\Delta_{ac1} = 0$, $\Delta_{ac2} = 0.1$, $\Gamma = 0.1$. All of the parameters are in units of Ω.

This work was partially supported by the National Natural Science Foundation of China (Nos. 11504104, 11447221, and 11274148), the Scientific Research Fund

of Hunan Provincial Education Department (No. 15C0539), the Natural Science Foundation of Hunan Province (No. 2015JJ6035), the National Natural Science Foundation of China for Fostering Talents in Basic Research (No. 11405052), and the Key Laboratory of Low Dimensional Quantum Structures and Quantum Control (No. QSQC1409).

References

1. A. Wallraff, D. I. Schuster, A. Blais, L. Frunzio, R. S. Huang, J. Majer, S. Kumar, S. M. Girvin, and R. J. Schoelkopf, Nature **431**, 162 (2004).
2. T. Yoshie, A. Scherer, J. Hendrickson, G. Khitrova, H. M. Gibbs, G. Rupper, C. Ell, O. B. Shchekin, and D. G. Deppe, Nature **432**, 200 (2004).
3. J. T. Shen and S. H. Fan, Phys. Rev. Lett. **95**, 213001 (2005).
4. T. Aoki, B. Dayan, E. Wilcut, W. P. Bowen, A. S. Parkins, T. J. Kippenberg, K. J. Vahala, and H. J. Kimble, Nature **443**, 671 (2004).
5. X. W. Xu, A. X. Chen, Y. Li, and Y. X. Liu, Phys. Rev. A **95**, 063808 (2017).
6. J. Zhao, L. Qin, X. Cai, Q. Lin, and Z. Wang, Chin. Opt. Lett. **15**, 050202 (2017).
7. W. B. Yan and H. Fan, Phys. Rev. A **90**, 053807 (2014).
8. C. H. Yan, L. F. Wei, W. Z. Jia, and J. T. Shen, Phys. Rev. A **84**, 045801 (2011).
9. L. Zhou, Z. R. Gong, Y. X. Liu, C. P. Sun, and F. Nori, Phys. Rev. Lett. **101**, 100501 (2008).
10. M. T. Cheng, J. P. Xu, and G. S. Agarwal, Phys. Rev. A **95**, 053807 (2017).
11. J. H. Li, R. Yu, C. L. Ding, and Y. Wu, Phys. Rev. A **93**, 023814 (2016).
12. R. Yu, J. H. Li, C. L. Ding, and X. X. Yang, Phys. Lett. A **375**, 2738 (2011).
13. J. Q. Liao and F. Nori, Sci. Rep. **4**, 6302 (2014).
14. D. E. Chang, A. H. Safavi-Naeini, M. Hafezi, and O. Painter, New J. Phys. **13**, 023003 (2011).
15. I. M. Mirza and S. J. van Enk, Phys. Rev. A **90**, 043831 (2014).
16. W. Chen and A. A. Clerk, Phys. Rev. A **89**, 033854 (2014).
17. L. G. Si, H. Xiong, M. S. Zubairy, and Y. Wu, Phys. Rev. A **95**, 033803 (2017).
18. M. Aspelmeyer, T. J. Kippenberg, and F. Marquardt, Rev. Mod. Phys. **86**, 1391 (2014).
19. P. Verlot, A. Tavernarakis, T. Briant, P. F. Cohadon, and A. Heidmann, Phys. Rev. Lett. **102**, 103601 (2009).
20. B. P. Abbott, R. Abbott, and T. D. Abbott, Phys. Rev. Lett. **116**, 061102 (2016).
21. I. Pikovski, M. R. Vanner, M. Aspelmeyer, M. S. Kim, and Č. Brukner, Nat. Phys. **8**, 393 (2012).
22. D. A. Golter, T. Oo, M. Amezcua, K. A. Stewart, and H. Wang, Phys. Rev. Lett. **116**, 143602 (2016).
23. J. M. Pirkkalainen, S. U. Cho, F. Massel, J. Tuorila, T. T. Heikkilä, P. J. Hakonen, and M. A. Sillanpää, Nat. Commun. **6**, 6981 (2015).
24. Z. Y. Xue, L. N. Yang, and J. Zhou, Appl. Phys. Lett. **107**, 023102 (2015).
25. X. X. Ren, H. K. Li, M. Y. Yan, Y. C. Liu, Y. F. Xiao, and Q. H. Gong, Phys. Rev. A **87**, 033807 (2013).
26. W. Z. Jia and Z. D. Wang, Phys. Rev. A **88**, 063821 (2013).
27. X. F. Zang, T. Zhou, B. Cai, and Y. M. Zhu, J. Opt. Soc. Am. B **30**, 1135 (2013).
28. X. Y. Yu and J. H. Li, J. Opt. Soc. Am. B **33**, 165 (2016).
29. H. Zhou, S. Che, P. Zuo, Y. Han, and D. Wang, Chin. Opt. Lett. **15**, 081401 (2017).